C.1.c.1.14-PREPARATION OF COPPER ALUMINUM-BIOCHAR COMPOSITE AS ADSORBENT OF MALACHITE GREEN IN AQUEOUS SOLUTION.pdf

By Risfidian Mohadi

WORD COUNT	5315	TIME SUBMITTED	22-JAN-2022 06:46AM
		PAPER ID	81669738

Journal of Engineering Science and Technology
Vol. 16, No. 1 (2021) 259 - 274

PREPARATION OF COPPER ALUMINUM-BIOCHAR COMPOSITE AS ADSORBENT OF MALACHITE GREEN IN AQUEOUS SOLUTION

NEZA R. PALAPA[1], TARMIZI TAHER[2], ARINI F. BADRI[1], SUHERYANTO[4], RISFIDIAN MOHADI[3,4], ADDY RACHMAT[4], ALDES LESBANI[1,3,*]

[1]Graduate School of Mathematics and Natural Sciences, Faculty of Mathematics and Natural Sciences, Universitas Sriwijaya, Jl. Palembang Prabumulih Km.32 Ogan Ilir 30662, Indonesia
[2]Institute of Regional Innovation, Hirosaki University, Matsubara 2-1-3, Aomori City, Aomori, Japan
[3]Research Center of Inorganic Materials and Coordination Complexes, Faculty of Mathematics and Natural Sciences, Universitas Sriwijaya, Jl. Palembang Prabumulih Km.32 Ogan Ilir 30662, Indonesia
[4]Department of Chemistry, Faculty of Mathematics and Natural Sciences, Universitas Sriwijaya, Jl. Palembang Prabumulih Km.32 Ogan Ilir 30662, Indonesia
*Corresponding Author: aldeslesbani@pps.unsri.ac.id

Abstract

In this work, CuAl/Biochar (BC) composite was prepared by the co-precipitation method. The materials were applied to remove malachite green in aqueous solution. These materials were characterized using XRD, FTIR, BET and SEM analyses. X-ray diffractograms confirmed the composite material with reflection (002) at 24° and new peaks at 1095 cm^{-1}. The BET result of CuAl/BC composite larger surface area is 168 m^2/g than 46 m^2/g for LDH. The adsorption study indicated the CuAl/BC composite follows pseudo-second-order (PSO) and Langmuir isotherm models. The maximum adsorption capacity of malachite green using CuAl/BC uptake is 164.316 mg/g. The thermodynamic analysis indicates that the malachite green adsorption is spontaneous, endothermic. The regenerative study of adsorbent CuAl/BC composite shows four times reused, and it still has high removal efficiency at 89 %.

Keywords: Adsorption, Biochar, CuAl/BC composite, Layered double hydroxide, Malachite green.

1. Introduction

The environmental issue becomes a severe problem and receives extensive attention in global society [1]. The main substances of environmental pollutants that come from human activities are organic dyes, metal ions, aromatic compounds, pesticides and drugs [2]. Generally, the dyes used in many industries such as paints, textiles, papers, cosmetics, and rubbers, resulted in the release of large amounts of coloured toxic effluent and contaminates water resources [3]. The practical and low-cost treatment to remove the dyes in water becomes more challenging because dye concentrations in effluent water need to be very low before releasing into the environment. Therefore, the complete removal of dye from effluents before their discharges into the surface water is necessary [4].

Several treatments method has been investigated regarding pollutants removals such as water oxidation [5], photodegradation [6], membrane separation [7], a biological process [8] and adsorption [9]. Among these methods, adsorption is more suitable in removing dyes from aqueous solutions. The adsorption is the easiest way, cheapest, effective method to remove dyes from solution and the adsorbent can be reused [10, 11]. Various materials have been examined and implemented as adsorbent to remove dyes from water such as bentonite [12], kaolinite [11], zeolite [13], montmorillonite [14] and layered double hydroxide [15].

Layered double hydroxide (LDH) is the anionic synthetic clay with general formula $[M2+1-xM3+x\ (OH)2]+xAx/n-n\ \cdot mH2O$ with M2+ containing divalent (Cu2+, Mg2+, Zn2+ and Ca2+) and M3+ containing trivalent metals ion (Al3+, Cr3+ and Fe3+) [16]. LDH has widely used as an adsorbent to remove heavy metals, organic compounds, and dyes from wastewater. Palapa et al. [17] reported that ZnAl LDH had been examined as an adsorbent to remove anionic dye such direct violet. On the other hand, ZnCr LDH has high efficiency in removing Cr (VI) metal ion in water [18]. The surface of LDH has a positive charge, LDH is considered as potential adsorbent for anionic dye. Several treatments were analysed to improve the adsorption activity for cationic dyes was carried out to modify LDH. According to Lesbani and co-workers [16] NiFe LDH has been modified by intercalation process using polyoxometalate to enhanced adsorptive removal of malachite green was 7.79 mg/g from 5.12 mg/g. The adsorption capacity of modified LDH is higher than pristine. The composites treatment also used to improve the adsorption capacity of cationic dyes by incorporation of carbon-based compounds such as biochar into LDH [19].

Biochar (BC) is a carbon-based compound from the pyrolysis of biomass at high temperatures. BC is an attractive carbon-rich material from Indonesian agricultural waste and industrial by-products that can be used in material modification [20]. BC has been known for its application on wastewater treatment, soil and sediment adsorption. Furthermore, BC has recently used as supporting materials [21, 22]. On the other hand, BC were reported used as an adsorbent to remove heavy metals [9, 23] and organic waste [20, 24, 25]. In the present work, CuAl LDH used to load BC and applied as malachite green removal. The adsorption study was determined using kinetic and thermodynamic parameters by varying time, temperature and initial concentration. The regeneration study carried out by desorption study.

2. Materials and Methods

2.1. Materials

The materials used were purchased from Merck and Sigma Aldrich with analytical grade purity > 99% such as copper nitrate, aluminum nitrate, sodium hydroxide, sodium carbonate without any purification. Biochar was obtained without the activation process from Bukata_organics (Sleman, Yogyakarta, Indonesia). All the pre-determined malachite green (MG) solutions prepared by dissolving the calculated amounts of MG into deionized water. Deionized water obtained from Purite water deionized purifying at Universitas Sriwijaya.

2.2. Methods

2.2.1. Preparation of CuAl/BC composite

In this work, the material of CuAl LDH was prepared by a facile co-precipitation method, as previously reported by Palapa and co-workers [15]. The composites material was made by mixing as much as 10 mL 0.75 M of copper nitrate with 10 mL 0.25 M aluminum nitrate. The mixture was under constant stirring for an hour until the complete dissolution of the starting materials. Another beaker containing 2 g of the biochar prepared and added into the mixture with continuous stirring. A solution of 1 M sodium hydroxide was added dropwise until pH 10. The mixing solution was kept at 80 °C for three days. Composites washed and dried afterward at room temperature for a day.

2.2.2. Adsorption and regeneration study

In this work, the adsorption experiments were conducted in the batch method under the constant stirring speed of 120 rpm. Typically, 0.05 g of the prepared material was contacted with 50 mL of MG solution previously prepared in various concentrations. The adsorption process was conducted by varying adsorption time, initial concentration, and adsorption temperature. The adsorption capacity of the material towards MG adsorption calculated by following Eq. (1).

$$q_e = \frac{(C_o - C_e)}{m} \cdot V \quad (1)$$

where q_e is the adsorption capacity of adsorbed material at the equilibrium (mg/g), C_o and C_e are the initial and equilibrium concentration of MG solution, respectively (mg/L). m is the amount of adsorbent (g). V is the volume of the used MG solution (L).

The regeneration of adsorbent conducted to investigate the effectivity of adsorbent regeneration. In this study, HCl 0.001 M was used as a reagent to the desorption process. The regeneration study carried out by 0.25 g of adsorbent into 0.1 L MG 150 ppm. The mixture was shaken for two hours. The adsorbent was separated from adsorbate, and adsorbate was read using UV-Vis spectrophotometer. The dried adsorbent reused for four cycles with a similar procedure.

3. Results and Discussion

3.1. Characterization

The CuAl LDH, BC and CuAl/BC composite were characterized by XRD Rigaku Miniflex-600 and the sample measured at scan rate 1 deg/min. The powder x-ray

diffraction pattern of CuAl LDH, BC and CuAl/BC composites are shown in Fig. 1(a). The XRD pattern of CuAl LDH shows a typical reflection of the layered LDH phase at 2θ 11°, 23°, 35°, and 59° that correspond to the (003), (006), (012), and (110) planes, respectively. The basal spacing of CuAl LDH correspond to (003) plane was 0.754 nm. The broad peaks of (002) plane in the diffraction pattern of BC are related to the presence of carbon and silica oxide groups. After being composites, all of the characteristic peaks in both pristine BC and CuAl LDH spectra appear in XRD pattern of CuAl/BC composite. The XRD pattern of CuAl/BC shows that the (003) plane that corresponds to the basal spacing of LDH shifted to the lower angle, i.e., 11.7o to 10.2o that indicates the composites of BC took place on interlayer and surface so that the reflection (003) was expanded from 0.754 nm to 0.857 nm.

Infrared spectra obtained from FTIR Shimadzu Prestige-21 measurement by KBr disc and the samples were scanned at wavenumber 400-4000 cm^{-1}. The FTIR spectra of CuAl, BC and CuAl/BC composite are presented in Fig. 1(b). The spectra of CuAl LDH showed the characteristic vibration band at a wavenumber of 3448 cm^{-1} and 1635 cm^{-1}, which correspond to the O-H stretching and bending vibration mode from water molecules. The sharp peak at 1381 cm^{-1} denotes the nitrate bending from anion within interlayer, which was reduced after being composites and vibration at 1095 appears as biochar characteristic.

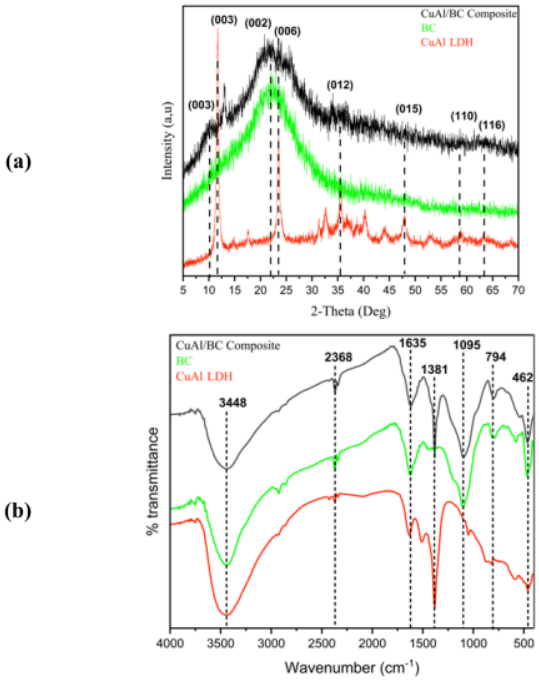

Fig. 1. Powder X-ray diffraction pattern (a) and FTIR spectrum (b) of CuAl LDH, BC and CuAl/BC composite.

The result of textural properties determination by using N2 adsorption-desorption method by Multipoint BET based on data collected by ASAP Micromeritics 2020 at 77 K presented in Table 1 while the adsorption isotherm shown in Fig. 2. The value of BET surface area, pore size and pore volume listed in Table 1 shows that the increase of the surface area and pore size of LDH after being composites by BC. The adsorption isotherms of each material are shown in Fig 2. The isotherm curve shows type IV with a typical hysteresis loop associated with capillary condensation within mesopore. The hysteresis curve of these materials resembles type H3. The H3 type hysteresis loop, according to IUPAC formed by an aggregate of a plate-like particle, which creates a slit-shaped pore of the mesopore type materials.

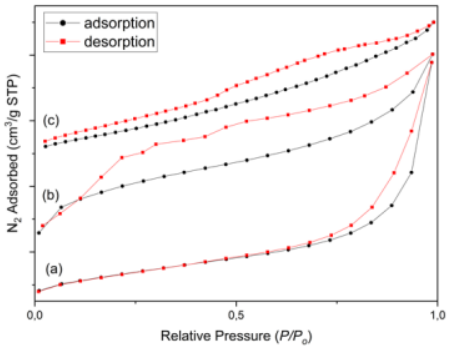

Fig. 2. Adsorption-desorption N_2 of (a) CuAl LDH, (b) CuAl/BC composite and (c) BC.

Table 1. Textural properties of CuAl LDH, BC and CuAl/BC composite.

Materials	BET Surface m^2/g	Pore Size nm	Pore Volume cm^3/g
BC	72.25	3.33	0.060
CuAl LDH	46.2	10.39	0.116
CuAl/BC composite	128.87	16.35	0.104

The surface morphology of materials characterized using SEM Quanta-650 Oxford instrument with the magnification size is 10 μm. The SEM images are shown in Fig. 3(a) depicts the morphologies of CuAl LDH, which indicates the agglomeration of particle. Figure 3(b) shows the pristine BC sample has a relatively bulky and pebble morphology, which can be related to the characteristic property of carbon material having a low specific surface area. The composite material shows both morphologies, as depicted by Fig. 3(c). Figure 3(c). shows that the composite surface is predominant on the surface of the composite of CuAl/BC LDH. The morphology of the composite shows the shaped structure of thin flakes. Gholami and others [26] also reported that the integration of Zn-Co-LDH with BC resulted in a regular-shaped formation. The particle size was calculated by ImageJ application, as shown in Fig. 4. The composite size reveals the diameter of thin flakes surface material and the higher frequency of composite material size is 0.2 μm. Furthermore, the composite material has a smaller particle size compare to CuAl pristine and BC,

the formation of aggregates is detected having a diameter size range of 1.8-18.2 µm. Thus, the average of CuAl/BC composite particle size is 3.34 µm.

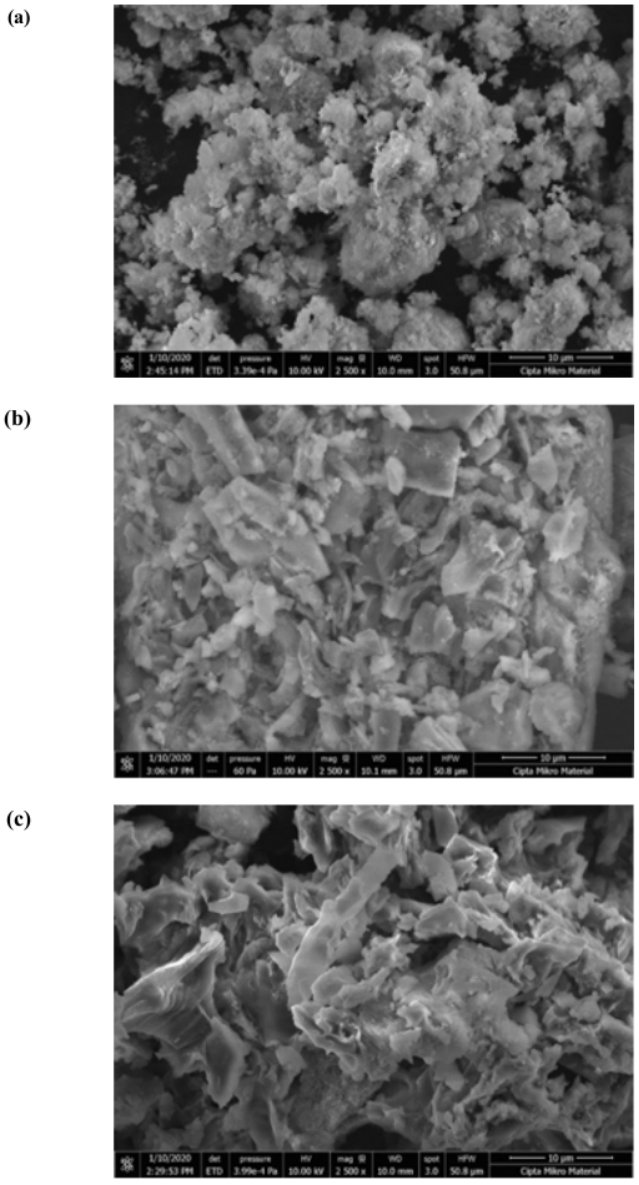

Fig. 3. SEM images of (a) CuAl LDH, (b) BC and (c) CuAl/BC composite.

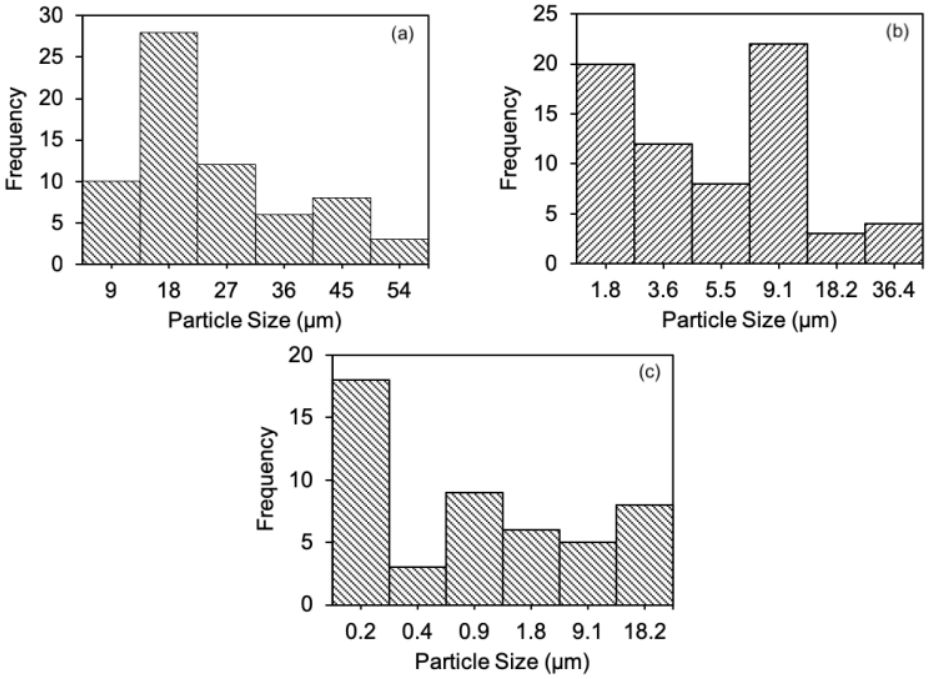

Fig. 4. The particles size distribution of (a) CuAl LDH, (b) BC and (c) CuAl/BC composite.

3.2. Adsorption study

The concentration of dye analyzed using UV-Visible spectrophotometer Bio-Base BK-UV1800. The maximum wavelength (λmax) of MG in acid and base solution was determined to get a better insight into the adsorption study. Figure 5(a) shows MG in the acidic condition, LDH displays high absorbance, which indicates the adsorption of MG did not occur well. This finding suggests that the active site of LDH is rich in cationic charge. According to Zhu and others [27] the adsorption of MG by LDH in the acidic condition causes the LDH structure to exfoliate, and the active site rich in positive charge prefers adsorbate with the opposite charge.

Figure 5(a) in base and normal condition, the adsorption occurs after stirring for an hour, resulting a lower absorbance value and showing that base condition of the adsorption is preferred because the active site of LDH is rich in OH- thus causing better adsorption of MG. Similar finding in Fig. 5(b) which indicated the higher adsorption in base condition. Figure 5(c). shows the adsorption of MG in acid condition is favourable; hence for CuAl/BC composite, adsorption carried out at acidic phase. Figure 5(c) suggests that in base and normal condition, adsorption by composite materials were shifted to a higher wavelength. This result assumes that the composite materials are causing the MG solution to become more alkaline. The scheme of changing pH shows in Fig. 6.

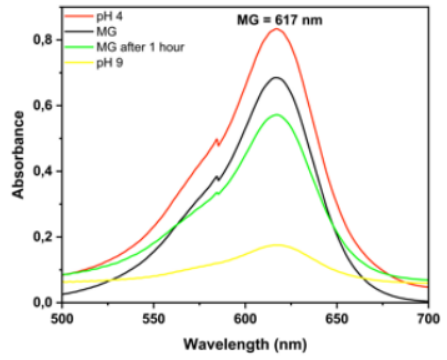

(a)

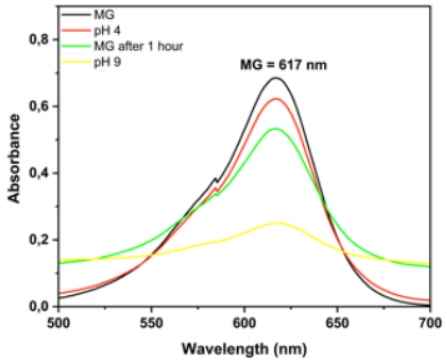

(b)

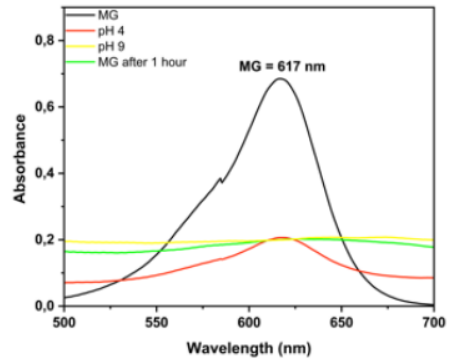

(c)

Fig. 5. UV-Visible spectra of MG adsorbed by (a) CuAl LDH, (b) BC and (c) CuAl/BC composite in acid and base solution.

The changing pH were indicated the removal of MG using these materials was affected by pH. According to Anbia and Ghaffari [28], due to a decrease in the system pH, the negatively charged adsorbent's site was reduced and the positive surface site was increased, which did not affability the adsorption of positively charged dye cations due to electrostatic repulsion. While the lower adsorption of MG at acidic pH is due to the presence of the excess H+ ions competing with dye cations onto the adsorbent's surface. Thus, the pH can be affected by the MG structure [29]. It may be due to the structural changes of MG molecules at high pH and increased over at base condition.

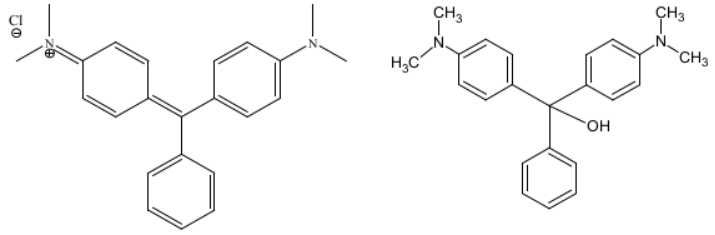

(a) **(b)**

Fig. 6. The scheme of changes in the structure of the MG in (a) 4<pH<6 and (b) pH>9.

The kinetic experiments of MG adsorption by CuAl LDH, BC and CuAl/BC composite increased rapidly with time were shown in Fig. 7. The CuAl/BC composite adsorbed higher than CuAl LDH and BC. During the first 90 minutes, all materials' adsorption process increased rapidly and reached 28 mg/g, 37 mg/g and 43 mg/g, respectively, due to the large amount of adsorption and reaches equilibrium in about 200 minutes. The adsorption capacity constantly stable over time because the active site of adsorbent fully occupied.

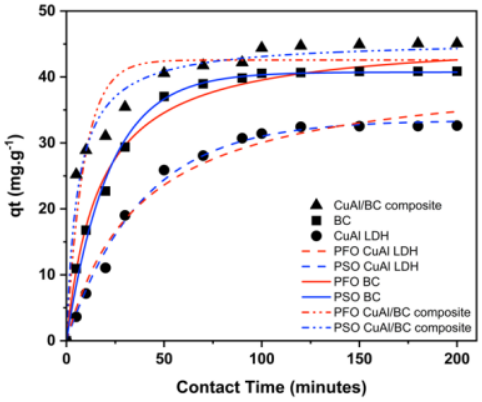

Fig. 7. Adsorption kinetic of MG on CuAl LDH, BC and CuAl/BC composite.

The pseudo first-order model (PFO) and pseudo second-order (PSO) model were applied to calculate the experimental kinetic data. These kinetic models can be expressed by the following Eqs. (2) and (3) [30];

$$\log(qe - qt) = \log qe - \frac{k_1 t}{2.303} \quad (2)$$

$$\frac{t}{qt} = \frac{1}{k_2\, qe^2} + \frac{1}{qe} t \quad (3)$$

with *qe* denotes adsorption capacity at equilibrium, k_1 is rate constant of PFO, k_2 is rate constant for PSO. The rate constant was obtained from plotting the equation to get correlation coefficients and listed in Table 2.

Table 2. The model parameters of adsorption kinetics.

Model	Adsorbents	$q_{e\,exp}$ (mg/g)	Parameter 1	Parameter 2	R^2
PFO	CuAl LDH	26.644	$q_{e\,calc}$ = 22.066 (mg/g)	k_1 = 0.0405	0.968
	BC	27.231	$q_{e\,calc}$ = 32.747 (mg/g)	k_1 = 0.0209	0.939
	CuAl/BC composite	28.175	$q_{e\,calc}$ = 18.477 (mg/g)	k_1 = 0.0340	0.963
PSO	CuAl LDH	26.644	$q_{e\,calc}$ = 30.156 (mg/g)	k_2 = 0.0012	0.996
	BC	27.231	$q_{e\,calc}$ = 31.525 (mg/g)	k_2 = 0.0016	0.978
	CuAl/BC composite	28.175	$q_{e\,calc}$ = 29.025 (mg/g)	k_2 = 0.0056	0.997

Table 2. represents the kinetic parameters obtained by plotting log(*qe-qt*) vs. t (PFO) and *t/qt* vs. *t* (PSO). The calculation result shows a coefficient correlation (R2) closed to one for all kinetic parameters. Based on Table 1, the kinetic model follows PSO with qe calc close to qe exp. The k_2 from this equation indicates the adsorbate mobilization more reactive and value of rate constant lower than k_1. CuAl/BC composite has a higher constant rate (k_2) than BC and CuAl LDH pristine. This finding indicates the good electrostatic attraction of MG and CuAl/BC cause the adsorption observed experimentally faster than others. Huang et al. [31] also reported that the kinetic model follows PSO indicate that the adsorption process is towards the physio-chemisorption rate-limit step. The isotherm model follows Langmuir and Freundlich were examined to simulate the adsorption of MG into CuAl LDH, BC and CuAl/BC composite. The Langmuir and Freundlich isotherm model equation are given as Eqs. (4) and (5).

$$\frac{Ce}{qe} = \frac{1}{q_{max}} C_e + \frac{1}{q_{max} k_L} \quad (4)$$

$$ln\ q_e = \ln k_F \frac{1}{n} \ln C_e \quad (5)$$

where *Ce* is initial concentration of adsorbate (mg/L); *qe* is adsorption capacity in saturated (mg/g); qmax is the maximum capacity of adsorbent (mg/g); *kL* and k_F are constant connected with affinity in bending sites of adsorbent; *n* is Freundlich linear constant. The value of n is more favourable if 0<n<2; if n>2 the adsorption

becomes hard [28]. Furthermore, the Langmuir equation assumed that the active site is homogeneous, and the adsorbent's interaction is low.

The effect of temperature and initial concentration are shown in Fig. 8. Figure 8 shows the increased temperature related to improving the adsorption capacity of the adsorbent. The higher adsorption capacity obtained by CuAl/BC composite in 323 K was 47.23 mg/g than CuAl LDH and BC (21.2 mg/g and 28.91 mg/g). However, the adsorption capacity of these adsorbents was increased with raising initial concentration and become stable after equilibrium. The result from Eqs. (3) and (4) were listed in Table 2. Based on the coefficient correlation (R^2) of the adsorption process, the isotherm models fitted Langmuir isotherm model and indicated the adsorption process might be a uniform monolayer. Table 3 showed the maximum adsorption capacity of Langmuir by CuAl/BC composite was 164.316 mg/g, which was higher with some previously reported in Table 4.

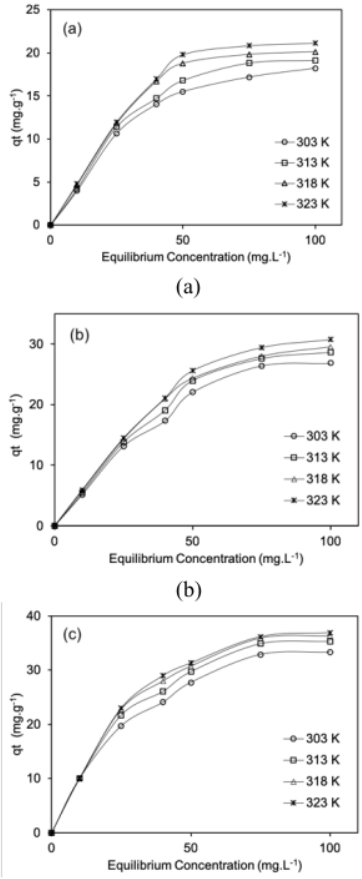

Fig. 8. Adsorption capacity vs. concentration in several temperatures of (a) CuAl LDH, (b) BC and (c) CuAl/BC composite.

Table 3. The model parameters of adsorption isotherm.

Adsorbent	T (K)	Langmuir			Freundlich		
		q_{max}	k_L	R^2	n	k_F	R^2
CuAl LDH	323	21.73	0.82	0.999	3.76	88.51	0.879
BC	323	31.25	0.94	0.999	3.02	13.38	0.957
CuAl/BC	323	164.31	0.38	0.999	8.42	22.99	0.994

Table 4. The comparison of MG adsorption using LDH, BC and composite.

Adsorbent	Time adsorption (min)	Qmax (mg/g)	Refs
$MnO_2/Al_2O_3/Fe_2O_3$ nanocomposite	120	99	[6]
Rice Husk BC	100	32.6	[29]
NiAl LDH	60	73.38	[30]
Sugarcane BC	51	10	[31]
CuCr LDH	60	59.2	[15]
Magnetic BC	180	127.3	[21]
Rice Husk-AC	20	63.85	[32]
CuAl/BC composite	90	164.316	This work

The thermodynamic parameter examined by the van't Hoff formula. The formula follows Eqs. (6) and (7).

$$\Delta G = -RT \ln (K_d) \quad (6)$$

$$\ln (K_d) = \frac{\Delta S}{R} - \frac{\Delta H}{RT} \quad (7)$$

R is constant gases (J/mol.K), and Kd is the adsorption distribution coefficient. The thermodynamic parameters for adsorption malachite green by CuAl LDH, BC and CuAl/BC composite are shown in Table 5. The thermodynamic parameters used to determine the nature of the adsorption process. The entropy (ΔS) and enthalpy (ΔH) process obtained from the linearity of ln (Kd) vs. T. Table 5. Shows the values of ΔH and ΔS are both positive. The positive ΔH values indicate that the adsorption process of MG onto CuAl/BC composite is endothermic. In contrast, the positive ΔS value suggests increasing randomness at the adsorbent-adsorbate interface during the adsorption process. The negative ΔG values showed the spontaneity of the adsorption process. Furthermore, it was found that ΔG value decreased with increasing the adsorption temperatures. It indicated that the adsorption process of malachite green for all adsorbents is more feasible at 323 K than 303 K.

The regeneration cycle of CuAl LDH, BC and CuAl/BC composite are shown in Fig. 9. To evaluate the economic value of adsorbent, the regeneration study determined in four cycles. Hence the desorption process was contacting an acidic reagent in low concentration, the results show the reusability process for composite material provides good removal efficiency, where the removal efficiency remains > 80 % after the fourth cycles. This result indicates the stability of the CuAl/BC composite is high and the desorption process does not distort the composite material

structure. However, the extreme decrease of CuAl LDH caused by the acidic reagent can be exfoliating LDH structure and dissolved due, not feasible to reuse [33].

Table 5. The thermodynamic parameters for adsorption malachite green by CuAl LDH, BC and CuAl/BC composite.

Adsorbent	T (K)	ΔG (kJ/mol)	ΔS (J/mol.K)	ΔH (kJ/mol)
CuAl LDH	303	-1.230	32.557	8.634
	313	-1.556		
	318	-1.719		
	323	-1.882		
BC	303	-1.216	33.441	8.916
	313	-1.551		
	318	-1.718		
	323	-1.885		
CuAl/BC composite	303	-0.464	18.767	5.222
	313	-0.652		
	318	-0.746		
	323	-0.840		

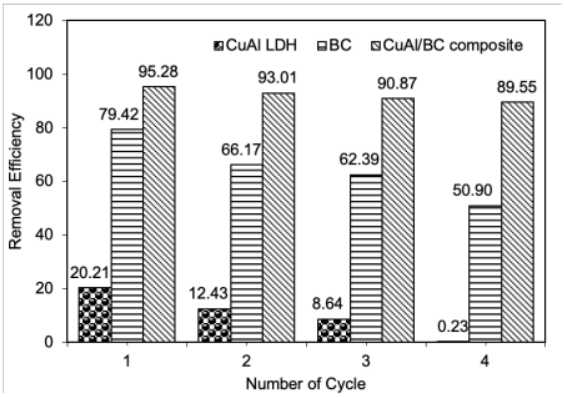

Fig. 9. Regeneration process of malachite green process by CuAl LDH, BC and CuAl/BC composite.

4. Conclusions

The CuAl/BC composite material has been successfully prepared and characterized. CuAl/BC composite was used as an adsorbent to remove the MG. The parameters of adsorption were determined using kinetic, isotherm, and thermodynamic parameters. The kinetic model of pseudo-second-order was appropriate for the composites with a coefficient correlation close to one. The

regeneration study showed that the fourth cycle adsorption process would reduce the adsorption capacity for LDH and BC significantly, but quietly for composites. The thermodynamic analysis indicates that the MG adsorption in CuAl/BC composite were spontaneous (ΔG<0); endothermic (18.767 kJ/mol); the randomness of solid-liquid phase interface (5.222 kJ/mol. The regeneration process was presented that after the adsorbent reused fourth times, the adsorption capacity of CuAl LDH and BC reduced significantly but not for the CuAl/BC composite.

Acknowledgment

Author would like to thanks to Universitas Sriwijaya, which provided funding through "*Hibah Profesi* dana PNPB" in the fiscal year 2020 for supporting the financial of this research. Special thanks to Research Centre of Inorganic Materials and Complexes FMIPA Universitas Sriwijaya for supporting analysis and instruments.

Nomenclatures

Greek Symbols

λ_{max}	Maximum wavelength
ΔG	Gibbs free energy
ΔH	Enthalpy
ΔS	Entropy

Abbreviations

BET	Brunauer-Emmett-Teller
IUPAC	International Union of Pure and Applied Chemistry
LDH	Layered Double Hydroxide
MG	Malachite Green
SEM	Scanning Electron Microscope

References

1. Shankar, Y.S.; Ankur, K.; Bhushan, P.; and Mohan, D. (2019). Utilization of water treatment plant (WTP) sludge for pretreatment of dye wastewater using coagulation/flocculation. *Advances in Waste Management*, 107-121.
2. Mourid, E.H.; Lakraimi, M.; Benaziz, L.; Elkhattabi, E.H.; and Legrouri, A. (2019). Wastewater treatment test by removal of the sulfamethoxazole antibiotic by a calcined layered double hydroxide. *Applied Clay Science*, 168, 87-95.
3. Kausar, A.; Iqbal, M.; Javed, A.; Aftab, K.; Nazli, Z.H.; Bhatti, H.N.; and Nouren, S. (2018). Dyes adsorption using clay and modified clay: a review. *Journal of Molecular Liquids*, 256, 395-407.
4. Starukh, H.; and Levytska, S. (2019). The simultaneous anionic and cationic dyes removal with Zn-Al layered double hydroxides. *Applied Clay Science*, 180, 1-5.
5. Kim, S.J.; Lee, Y.; Lee, D.K.; Lee, J.W.; and Kang, J.K. (2014). Efficient Co-Fe layered double hydroxide photocatalysts for water oxidation under visible light. *Journal of Materials Chemistry A*, 2(12).
6. Logita, H.H.; Tadesse, A.; and Kebede, T. (2015). Synthesis, characterization and photocatalytic activity of $MnO_2/Al_2O_3/Fe_2O_3$ nanocomposite for

degradation of malachite green. *African Journal of Pure and Applied Chemistry*, 9(11), 211-222.

7. Xu, Y.; Li, Z.; Su, K.; Fan, T.; and Cao, L. (2018). Mussel-inspired modification of PPS membrane to separate and remove the dyes from the wastewater. *Chemical Engineering Journal*, 341, 371-382.
8. Robinson, T.; McMullan, G.; Marchant, R.; and Nigam, P. (2001). Remediation of dyes in textile effluent: a critical review on current treatment technologies with a proposed alternative. *Bioresource Technology*, 77(3), 247-255.
9. Silos-Llamas, A.K.; Durán-Jiménez, G.; Hernández-Montoya, V.; Montes-Morán, M.A.; and Rangel-Vázquez, N.A. (2020). Understanding the adsorption of heavy metals on oxygen-rich biochars by using molecular simulation. *Journal of Molecular Liquids*, 298.
10. Foroutan, R.; Mohammadi, R.; Razeghi, J.; and Ramavandi, B. (2019). Performance of algal activated carbon/Fe_3O_4 magnetic composite for cationic dyes removal from aqueous solutions. *Algal Research*, 40.
11. Abidi, N.; Duplay, J.; Jada, A.; Errais, E.; Ghazi, M.; Semhi, K.; and Trabelsi-Ayadi, M. (2019). Removal of anionic dye from textile industries' effluents by using Tunisian clays as adsorbents. Zeta potential and streaming-induced potential measurements. *Comptes Rendus Chimie*, 22(2-3), 113-125.
12. Taher, T.; Rohendi, D.; Mohadi, R.; and Lesbani, A. (2019). Congo red dye removal from aqueous solution by acid-activated bentonite from sarolangun: kinetic, equilibrium, and thermodynamic studies. *Arab Journal of Basic and Applied Sciences*, 26(1), 125-136.
13. Oliveira, J.A.; Cunha, F.A.; and Ruotolo, L.A.M. (2019). Synthesis of zeolite from sugarcane bagasse fly ash and its application as a low-cost adsorbent to remove heavy metals. *Journal of Cleaner Production*, 229, 956-963.
14. Jiang, D.B.; Jing, C.; Yuan, Y.; Feng, L.; Liu, X.; Dong, F.; Dong, B.; and Zhang, Y.X. (2019). 2D-2D growth of NiFe LDH nanoflakes on montmorillonite for cationic and anionic dye adsorption performance. *Journal of Colloid and Interface Science*, 540, 398-409.
15. Palapa, N.R.; Mohadi, R.; Rachmat, A.; and Lesbani, A. (2020). Adsorption study of malachite green removal from aqueous solution using Cu/M3+ (M3+= Al,Cr) layered double hydroxide. *Mediterranean Journal of Chemistry*, 10(1), 33-45.
16. Lesbani, A.; Taher, T.; Palapa, N.R.; Mohadi, R.; Rachmat, A.; and Mardiyanto. (2020). Preparation and utilization of Keggin-type polyoxometalate intercalated Ni-Fe layered double hydroxides for enhanced adsorptive removal of cationic dye. *SN Applied Sciences*, 2.
17. Palapa, N.R.; Taher, T.; Mohadi, R.; and Lesbani, A. (2019). Kinetic aspect of direct violet adsorption on M2+/M3+ (M2+: Zn; M3+: Al, Fe, Cr) layered double hydroxides. *Proceedings of the 2nd International Conference on Science, Mathematics, Environment and Education*. Solo City, Indonesia, 2194(1).
18. Oktriyanti, M.; Palapa, N.R.; Mohadi, R.; and Lesbani, A. (2019). Modification of Zn-Cr layered double hydroxide with keggin ion [α-SiW12O40] 4− as Cr(VI) adsorbent. *Indonesian Journal of Environmental Management and Sustainability*, 3(3), 93-99.

19. Moyo, L.; Focke, W.W.; Heidenreich, D.; Labuschagne, F.J.W.J.; and Radusch, H.J. (2013). Properties of layered double hydroxide micro- and nanocomposites. *Materials Research Bulletin*, 48(3), 1218-1227.
20. Tareq, R.; Akter, N.; and Azam, M.S. (2019). Biochars and biochar composites: low-cost adsorbents for environmental remediation. *Biochar from Biomass and Waste*, 169-209.
21. Huang, Q.; Song, S.; Chen, Z.; Hu, B.; Chen, J.; and Wang, X. (2019). Biochar-based materials and their applications in removal of organic contaminants from wastewater: state-of-the-art review. *Biochar*, 1(1), 45-73.
22. Gholami, P.; Khataee, A.; Soltani, R.D.C.; Dinpazhoh, L.; and Bhatnagar, A. (2020). Photocatalytic degradation of gemifloxacin antibiotic using Zn-Co-LDH@biochar nanocomposite. *Journal of Hazardous Materials*, 382.
23. Ni, B.; Huang, Q.; Wang, C.; Ni, T.; Sun, J.; and Wei, W. (2019). Competitive adsorption of heavy metals in aqueous solution onto biochar derived from anaerobically digested sludge. *Chemosphere*, 219, 351-357.
24. Meili, L.; Lins, P.V.; Zanta, C.L.P.S.; Soletti, J.I.; Ribeiro, L.M.O.; Dornelas, C.B.; Silva, T.L.; and Veira, M.G.A. (2019). MgAl-LDH/biochar composites for methylene blue removal by adsorption. *Applied Clay Science*, 168, 11-20.
25. Taghizadeh-Toosi, A.; Clough, T.J.; Sherlock, R.R.; and Condron, L.M. (2012). Biochar adsorbed ammonia is bioavailable. *Plant and Soil*, 350(1), 57-69.
26. Gholami, P.; Dinpazhoh, L.; Khataee, A.; Hassani, A.; and Bhatnagar, A. (2019). Facile hydrothermal synthesis of novel Fe-Cu layered double hydroxide/biochar nanocomposite with enhanced sonocatalytic activity for degradation of cefazolin sodium. *Journal of Hazardous Materials*, 381.
27. Zhu, Y.; Rong, J.; Zhang, T.; Xu, J.; Dai, Y.; and Qiu, F. (2018). Facile and controlled fabrication of Cu-Al layered double hydroxide nanosheets/laccase hybrid films: a route to efficient biocatalytic removal of congo red from aqueous solutions. *ACS Applied Nano Materials*, 1(1), 284-292.
28. Anbia, M.; and Ghaffari, A. (2011). Removal of malachite green from dye wastewater using mesoporous carbon adsorbent. *Journal of the Iranian Chemical Society*, 8(1), 67-76.
29. Maurya, N.S.; Mittal, A.K.; Cornel, P.; and Rother, E. (2006). Biosorption of dyes using dead macro fungi: effect of dye structure, ionic strength and pH. *Bioresource Technology*, 97(3), 512-521.
30. Qu, W.; Yuan, T.; Yin, G.; Xu, S.; Zhang, Q.; and Su, H. (2019). Effect of properties of activated carbon on malachite green adsorption. *Fuel*, 249, 45-53.
31. Huang, D.; Liu, C.; Zhang, C.; Deng, R.; Wang, R.; Xue, W.; Luo, H.; Zheng, G.; Zhang, Q.; and Guo, X. (2019). Cr(VI) removal from aqueous solution using biochar modified with Mg/Al-layered double hydroxide intercalated with ethylenediaminetetraacetic acid. *Bioresource Technology*, 276, 127-132.
32. Leng, L.; Yuan, X.; Zeng, G.; Shao, J.; Chen, X.; Wu, Z.; Wang, H.; and Peng, X. (2015). Surface characterization of rice husk bio-char produced by liquefaction and application for cationic dye (malachite green) adsorption. *Fuel*, 155, 77-85.
33. Saha, P.; Chowdhury, S.; Gupta, S.; and Kumar, I. (2010). Insight into adsorption equilibrium, kinetics and thermodynamics of Malachite Green onto clayey soil of Indian origin. *Chemical Engineering Journal*, 165(3), 874-882.

C.1.c.1.14-PREPARATION OF COPPER ALUMINUM-BIOCHAR COMPOSITE AS ADSORBENT OF MALACHITE GREEN IN AQUEOUS SOLUTION.pdf

ORIGINALITY REPORT

0%

SIMILARITY INDEX

PRIMARY SOURCES

EXCLUDE QUOTES	OFF	EXCLUDE MATCHES	< 5%
EXCLUDE BIBLIOGRAPHY	ON		